Third International Conference on 3D Imaging and Modeling, Quebec, Canada, May 28-June 1, 2001. pp. 179-186.

A Method for the Registration of Attributed Range Images

Guy Godin

Visual Information Technology Group
National Research Council of Canada
Bldg. M-50, 1500 Montréal road
Ottawa (Ontario), Canada K1A 0R6
guy.godin@nrc.ca

Denis Laurendeau Robert Bergevin

Computer Vision and Systems Laboratory
Dept. of Electrical and Computer Engineering
Laval University
Québec (Québec), Canada G1K 7P4
{laurend,bergevin}@gel.ulaval.ca

Abstract

Registration of range images requires the identification of common portions of surfaces between which a distance minimization is performed. This paper proposes a framework for the use of dense attributes of range image elements as a matching constraint in the registration. These attributes are chosen to be invariant to rigid transformations, so that their value is similar in different views of the same surface portion. Attributes can be derived from the geometry information in the range image, such as surface curvature, or be obtained from associated intensity measurements. The method is based on the Iterative Closest Compatible Point algorithm augmented with a random sampling scheme that uses the distribution of attributes as a guide for point selection. Distance minimization is performed only between pairs of points considered compatible on the basis of their attributes. The performance of the method is illustrated on a rotationally symmetric object with color patterns.

1. Introduction

Registration of a set of range images is defined as the process of recovering, for each image in the set, the 3-D rigid transformation (rotation and translation) with regards to the sensor that brings the image points into a common object-centered Cartesian coordinate system. This task is usually accomplished by setting the problem as an optimization: the cost function is based on a metric estimating the distance between the common portions of a surface measured in different views. This optimization problem is generally non-convex, and the various methods that have been proposed in the computer vision literature differ by the formulation of the inter-surface metric as well as the minimization techniques employed. Obviously, registration of images from the measured data can only be achieved if there is a common surface area visible in the different images to be registered. If the correspondences between points in different images were known a priori, the solution to registration would be direct. Therefore, the essential difficulty of registration resides in the identification of regions in different images corresponding to the same surface area.

The method described in this paper uses attributes of individual range image elements to assist in the process of identification of common portions of surfaces. The attributes form a dense feature field that constrains potential matches to pairs of similar points. Attributes are defined as vectors attached to each element of the range image. Since different images are taken from different and unknown relative points of view, the type of attributes must be chosen to be viewpoint-invariant: a given surface point on a sensed object should in principle possess the same attribute value in the different images in which it is visible. Such attributes may be derived from the geometry information or from additional measurements, such as reflected intensities.

This paper presents a framework for the use of attributes in the registration of a pair of range images. It is set up as an extension of the Iterative Closest Point method [4] that incorporates local attributes as a constraint on the matching of the closest points, coupled with a random sampling scheme guided by the distribution of attributes for the identification of common surface areas.

1.1. Related work

Other registration techniques incorporating attributes have been proposed before. In [17], a curvature sign map is computed and segmented into regions of similar sign classes. These regions are organized as an attributed graph; a subgraph matching algorithm is then applied to recover the correspondence and the 3-D transformation. Range images triangulated at multiple resolutions can be registered using a technique that filters potential matches between triangles based on their geometric features [2]. A general method for integrating information between successive

frames [8] relies on local feature vectors in order to identify correspondences. In [23], local estimates of the Darboux frames are used to find consistent motion estimates between surface patches. A method for rigid and affine registration [7] uses principal curvature and frames, as seed for initial estimate as well as in the augmented distance function to be minimized. A modification to the Iterative Closest Point (ICP) method enforces an attribute-based compatibility constraint (color-based attributes [10] and curvature classes [11]) in the pairing while keeping an Euclidian distance metric. In [14], color information is integrated in the refinement step of an ICP algorithm, by computing a distance function that adds distance in color space to the Euclidian distance. A similar method is discussed in [22]. A matching constraint based on color is applied to 3-D points following an alignment based on 2-D warping of the attached color image, combined with a random sampled 3-D registration approach [19]. In [21], a sparse set of feature points is identified in the intensity channel of a range image and used as the vertices of a Delauney tetrahedrization; the rigid transformation between images is estimated by matching triangles of similar shapes and compatible vertices. The intensity image is exploited in [24] to compute gradients that assist in the range image pairing process. A related technique for range flow computation is proposed in [25].

The new method proposed in this paper addresses the problem of registration from arbitrary initial relative poses, not just of refinement. It is described in terms of generic attributes, but a particular example is provided which uses reflectance parameters estimated from range and color images.

2. Attributed range images

An attributed range image R_i is defined as a two-dimensional array where each element $\mathbf{r}_i(\mathbf{u}_j)$, called a *rigel* (for *range image element*), is composed of the 3-D Cartesian coordinate $\mathbf{p}_i(\mathbf{u}_j)$ of the measured surface point as well as a m-dimensional attribute vector $\mathbf{a}_i(\mathbf{u}_j)$. It should be noted that some positions in the array may be empty, corresponding to shadow or dropout points, or points removed by background thresholding, for example. Thus n_i, the actual number of valid elements in R_i, is less than or equal to the number of elements of the array.

The attribute vector $\mathbf{a}_i(\mathbf{u}_j)$ attached to each element $\mathbf{r}_i(\mathbf{u}_j)$ can be: (i) derived from the measured geometric information $\mathbf{p}_i$ (e.g. principal curvatures), (ii) computed from additional information such as the intensity channel(s) of the range sensors, or (iii) a combination of both. The attribute values may belong to a finite set of *discrete* labels, or correspond to samples of a *continuous* function.

2.1. Intensity-based attributes

Most active optical range sensors provide, in addition to surface coordinates, a measurement of the amount of light reflected towards the sensor at each sensed point. This k-channel information is usually referred to as *intensity*. For a monochromatic laser sensor, k is equal to one, while $k = 3$ for range sensors that integrate trichromatic imaging. Alternately, an auxiliary imaging sensor and light source may be used. These measurements are a function of the reflective properties of the surface as well as its relative position and orientation with regards to the sensor. To be used as an invariant attribute, they must be transformed into a m-dimensional quantity that is independent, at least in principle, of the pose of the object relative to the sensor.

A first possible approach is to extract the intrinsic surface reflectance parameters by inverting an illumination model. The geometric measurements of the surface provide information on relative distance and orientation of the surface, and the direction of illumination and observation are known since they are controlled as part of the range sensing process. Such a method is described in [1]. It computes the parameters of a dichromatic model, composed of the sum of a body (or diffuse) and a surface (or specular) component. The diffuse reflection coefficients are computed for each point, after removal of the specular part which is hypothesized to have locally uniform parameters. These coefficients are more computationally stable than the specular parameters and are usually more locally discriminating. In this case, m (the dimensionality of the attributes) is equal to the number of intensity channels k. Other methods for reflectance parameter extraction can be found in [13, 16].

Attributes can be computed without the requirement of sensor and reflectance modelling in cases where $k > 1$. The intensity vector can be projected into a lower dimensional space, in an attempt to compensate for viewpoint-dependent intensity changes. One possibility is to use the hue-saturation space, which eliminates the surface orientation attenuation on a purely Lambertian surface, or even only hue. However this approach, which results in $m < k$, may create potential ambiguities in the matching.

In a minimal scheme, the intensity can be transformed into a set of discretized labels, such as edge marks, points of interest such as corners, or color clusters. In such cases, $m = 1$ and $\mathbf{a}_i$ is discrete.

2.2. Local curvature attributes

Local curvature information has been used in various ways in range image analysis. The principal frame (surface normal, principal directions and curvatures) provides in itself enough information to constrain the rigid transformation between two points to two possibilites (except at

umbilic points) [23, 7]. In the framework presented here, the attributes must represent quantities that are independent of the coordinate system. Clearly, the normal and principal directions are not. However the magnitudes of the principal curvatures are, and can be used in two ways: as a continuous 2-dimensional attribute, or as one of the set of eight curvature labels based on the signs of mean and Gaussian curvatures [3]. The curvature computation method should itself be invariant as much as possible to the viewpoint: such a method is described in [6] and used as part of a registration method in [11].

3. Iterative closest compatible point

The Iterative Closest Point (ICP) method [4] is designed for registration of a set of 3-D points X_i to a 3-D reference surface S. It is assumed that all the points X_i belong to S. The method is shown to converge monotonically to a local minimum. For a pair of range images, the registration problem differs since one image is in general not a subset of the other. Hence, modifications are required to prevent points of one image that have no counterpart in the other from biasing the solution. For example, an adaptive distance threshold was proposed in [26]. A method based on random sampling and LMS estimation [18] addresses this problem by randomly selecting small subsets of one image and applying the standard ICP method with regards to the second image.

The Iterative Closest Compatible Point (ICCP), first proposed in [10, 11], differs from the ICP by searching for the closest point under a constraint of similarity in attributes (diffuse reflectance [10] or curvature sign classes [11]). Other methods (e.g. [7, 14, 22]) use attributes in the matching by incorporating them in a $(3+m)$-dimensional distance metric $\mathcal{D}^2_\lambda$ in the form:

$$\mathcal{D}^2_\lambda(\mathbf{r}_1, \mathbf{r}_2) = \|\mathbf{p}_2 - \mathbf{p}_1\|^2 + \sum_{i=1}^{m} \lambda_i (a_{2i} - a_{1i})^2 \qquad (1)$$

where $\mathbf{a}_j = (a_{j1}, ..., a_{jm})$. Instead, the ICCP uses the attributes as a compatibility measure, acting as an acceptance/rejection filter on potential pairings. This approach avoids the difficulty of choosing the values of λ_i for balancing the distance metric between Euclidian and attribute spaces. Moreover, the pairing process is not skewed by systematic biases in computed attributes, as long as the bias is within the defined limits of compatibility. Attributes also constrain the search space in the closest point determination to subsets of potentially compatible points, therefore improving the most computationally expensive operation in an ICP-type registration algorithm.

In general it cannot be considered that one image is a subset of the other, contrary to the image-to-model registration problem originally addressed in [4]. The formulation of the algorithm should therefore be commutative, that is, it should in principle yield the same result independent of the order in which the images in a pair are considered. This commutativity requirement [26, 10] is satisfied by minimizing the distance of points $\mathbf{r}_1(\mathbf{u}_i) \in R_1$ to compatible points of R_2, as well as $\mathbf{r}_2(\mathbf{u}_i) \in R_2$ to compatible points of R_1.

Since the compatibility measure is invariant to rigid transformations, and therefore does not change through the iterations, the ICCP can be interpreted as a set of rigidly coupled ICP subproblems between subsets of mutually compatible points. When all points share equal (or at least compatible) attributes, the ICCP is equivalent to the traditional ICP. It can be shown [10] that the basic ICCP has the same monotonic convergence property as the ICP. But it also suffers in the same manner from the effects of portions of surface appearing in only one of the images: in [10], a distance influence function is applied (at the cost of a loss of the monotonic convergence property) to partially address this problem. Any additional technique for acceleration and pruning of bad matches that have been proposed for ICP-type registration can be applied under the ICCP formalism.

4. Random sampled ICCP

The new method presented here extends the LMS-type method of [18] to the case of a pair of attributed range images, using an ICCP-type method. Attributes play two roles in the proposed method: first their distribution orients the selection of random samples; secondly the determination of the closest point is constrained by attribute compatibility as with the ICCP. The registration procedure is applied to a number of subsets and the computed transformation is evaluated. The transformation with the best Least Median of Squares score is kept. The best estimate is then refined using the inlier points in both images.

4.1. Algorithm

Four basic operations are required by the algorithm:

- A random sample selector $\mathcal{H}(n_c, R_i, H(\mathbf{a}))$ selects n_c rigels from R_i according to their attributes, following a probability distribution specified by the m-dimensional probability density function $H(\mathbf{a})$
- A Boolean compatibility test $\mathcal{C}(\mathbf{r}_i(\mathbf{u}_m), \mathbf{r}_j(\mathbf{u}_n))$ determines the compatibility of the attributes of two rigels $\mathbf{r}_i(\mathbf{u}_m)$ and $\mathbf{r}_j(\mathbf{u}_n)$
- The function $\mathcal{D}(\mathbf{r}_i(\mathbf{u}_m), \mathbf{r}_j(\mathbf{u}_n))$ represents the Euclidian distance between the geometric components of two rigels $\|\mathbf{p}_i(\mathbf{u}_m) - \mathbf{p}_j(\mathbf{u}_n)\|$
- The closest compatible point selection function $\mathcal{F}(\mathbf{r}_i(\mathbf{u}_m), R_j)$ finds the rigel $\mathbf{r}_j(\mathbf{u}_{mp}) \in R_j$

such that, for all the rigels $\mathbf{r}_j(\mathbf{u}_k) \in R_j$ satisfying $\mathcal{C}(\mathbf{r}_i(\mathbf{u}_m), \mathbf{r}_j(\mathbf{u}_k))$, $\mathcal{D}(\mathbf{r}_i(\mathbf{u}_m), \mathbf{r}_j(\mathbf{u}_{mp})) \leq \mathcal{D}(\mathbf{r}_i(\mathbf{u}_m), \mathbf{r}_j(\mathbf{u}_k))$

In general, $\mathcal{F}$ may fail when no elements of R_j are compatible with $\mathbf{r}_i(\mathbf{u}_m)$. However, the biased random sampling function $\mathcal{H}$ will be constructed in a way that ensures the selection of rigels that are compatible with at least one rigel in the other image. More details on the particular forms of $\mathcal{H}$, $\mathcal{C}$ and $\mathcal{F}$ are provided in the following subsections.

For clarity, the algorithm is stated in two parts: procedure αRSICCP performs the registration of random sampled subsets; procedure RSICCP iterates over a number of subsets, selects the best results, and refines the estimate using the subsets in both images that are identified as inliers.

Procedure αRSICCP:

- Data: two attributed range images R_1 and R_2; an initial estimate of the rigid transformation $\mathbf{T}_{ini}$ that brings R_1 onto R_2

0. Initialization: $k := 0$; $\mathbf{T}_0 := \mathbf{T}_{\text{ini}}$
1. Construct the random selection probability density function $H(\mathbf{a}_i)$ *(see Sect. 4.2)*
2. Select N_{C1} rigels $\mathbf{r}_{S1}(\mathbf{u}_i)$ using $\mathcal{H}(N_{C1}, R_1, H)$
3. Select N_{C2} rigels $\mathbf{r}_{S2}(\mathbf{u}_i)$ using $\mathcal{H}(N_{C2}, R_2, H)$
4. Do:
    1. $k := k + 1$
    2. For each rigel $\mathbf{r}_{S1}(\mathbf{u}_i)$, find the closest compatible point $\mathbf{r}_{C2}(\mathbf{u}_{j_i})$ in R_2 using $\mathcal{F}(\mathbf{T}_{k-1}\mathbf{r}_{S1}(\mathbf{u}_i), R_2)$
    3. For each rigel $\mathbf{r}_{S2}(\mathbf{u}_i)$, find the closest compatible point $\mathbf{r}_{C1}(\mathbf{u}_{j_i})$ in R_1 using $\mathcal{F}(\mathbf{T}_{k-1}^{-1}\mathbf{r}_{S2}(\mathbf{u}_i), R_1)$
    4. Let the distance measure between the two images for a given transformation $\mathbf{T}_k$:

$$e_k = \frac{1}{N_{C1}+N_{C2}} \cdot \left(\sum_{i=1}^{N_{C1}} \mathcal{D}^2(\mathbf{T}_k\mathbf{r}_{S1}(\mathbf{u}_i), \mathbf{r}_{C2}(\mathbf{u}_{j_i})) + \sum_{i=1}^{N_{C2}} \mathcal{D}^2(\mathbf{r}_{S2}(\mathbf{u}_i), \mathbf{T}_k\mathbf{r}_{C1}(\mathbf{u}_{j_i})) \right) \quad (2)$$

    5. Compute $\mathbf{T}_k$ that minimizes e_k

Until: Convergence test succeeds

- Result: $\mathbf{T}_{\text{final}} := \mathbf{T}_k$ is the estimated transformation bringing R_1 towards R_2.

Here, the application of a rigid transformation $\mathbf{T}$ to a range image element $\mathbf{r}_i(\mathbf{u}_j)$ must be understood to mean its application to the geometric component $\mathbf{p}_i(\mathbf{u}_j)$ only. At each iteration, $\mathbf{T}_k$ represents the total transformation between R_1 and R_2, to avoid error cumulation from the incremental transformations. The rigid transformation minimizing e_k for a set of paired points is computed using the method in [12].

In procedure RSICCP, the αRSICCP procedure is repeated N_T times. Each of the N_T estimated transformations is evaluated by computing the median of the sum of squared distance to the closest compatible point, if any, for all elements in R_1 and R_2. The best transformation is applied, points on the overlapping area are identified by thresholding, and iterations of the basic ICCP [10] are then run:

Procedure RSICCP:

- Data: two attributed range images R_1 and R_2; an initial estimate (or an hypothesis) of the rigid transformation $\mathbf{T}_{ini}$ that brings R_1 onto R_2

0. Initialization: $B := \infty$ *; least median of error*
1. Do N_T times:
    1. Invoke procedure αRSICCP; result $\rightarrow \mathbf{T}_\alpha$
    2. $b :=$ median of
$$\{\mathcal{D}(\mathbf{T}_\alpha\mathbf{r}_{1i}, R_2)\} \cup \{\mathcal{D}(\mathbf{r}_{2i}, \mathbf{T}_\alpha R_1)\}$$
    3. if $b < B$ then $B := b, \mathbf{T}_B := \mathbf{T}_\alpha$
2. Select subsets R_{S1} and R_{S2} of R_1 and R_2 containing points for which $\mathcal{D}(\cdot) < h\ \sigma$, where $\sigma = 1.4826\ B$ and h is a predefined threshold
3. Refine transformation by performing ICCP between R_{S1} and R_{S2}, using $\mathbf{T}_B$ as initial estimate; result $\rightarrow \mathbf{T}_f$

- Result: $\mathbf{T}_f$

As with all data-driven registration, proper convergence of the method depends on the initial configuration of the two images, their geometry, and the distribution of attributes. It may also be necessary to explore a space of initial transformations, in which case the procedure RSICCP is invoked with a number of different $\mathbf{T}_{ini}$, and the best transformation is selected according to the value of B across the different runs.

By far the most computationally expensive part of Step 1 of RSICCP is the computation of the median of residual distances (Step 1.2). Instead of using a closest point search, some authors [5, 18, 15, 19, 9] argue for the use of distance along predetermined projection lines (such as surface normals or lines of sight) for the evaluation of the quality of registration. However, this approach only considers the geometric quality of the registration, since the projection ignores attribute compatibility. One possible solution is proposed in [19]: the difference in attribute ((r, g, b) triplets in this case) is used to accept the pairs aligned by projection. But the method is used after an initial alignment through image warping, thus the registration of the color channels can be considered to be very good, and therefore most pairs are properly aligned in 2D. However, since the goal of RSICCP is to estimate registration from an arbitrary initial pose, such a condition does not exist. Therefore the distance to the closest compatible point is preferred as the registration metric, even though it is more computationally expensive. The selection threshold is defined as h times (e.g. $h = 2.5$) the estimated variance σ, itself estimated from the median using the 1.4826 correction factor for large population size, assuming less that 50% of outliers.

4.2. Random point selection $\mathcal{H}$

The first step in the algorithm is the selection of random subsets of rigels using $\mathcal{H}$. The underlying assumption in random sampling methods is that at least one of the selected subsets will be composed only of inliers. In the context of registration, inliers are defined as points that belong to portions of surface common to both images. The distribution of attributes in R_1 and R_2 is used to guide the random selection towards rigels whose attribute values appear in both images, as an indication of the possibility that they belong to an area of the object common to the two images.

The selection process is guided by the m-dimensional probability density function H defined as:

$$H(\mathbf{a}) = \min(H_1(\mathbf{a}), H_2(\mathbf{a})) \tag{3}$$

where $H_1(\mathbf{a})$ and $H_2(\mathbf{a})$ are the normalized m-dimensional p.d.f. for the attributes of elements in R_1 and R_2, respectively.

One property of random selection under the distribution H is that rigels with attributes appearing more often in both images are preferred in the selection. Furthermore, assuming there is no noise in the attributes, all elements selected in the subset are ensured to have at least one compatible counterpart in the other image, since otherwise the value of H for that attribute would be zero. The unavoidable presence of noise in estimated attributes is addressed in the implementation.

In practice, discrete classes are used when attributes belong to a continuous function: the attribute p.d.f. for each image is approximated by a histogram constructed by accumulating attribute occurences in classes corresponding to fixed intervals in each of the m dimensions. This binning compensates for the presence of noise in attributes, given that their size exceeds that of the noise. A more accurate - but much more expensive - method for constructing H would find, for each rigel in one image, the actual number of compatible rigels in the other image. For discrete attributes, these classes are readily determined on the basis of their labels.

The random selection operates as follows: an attribute value is generated by transforming a uniformly distributed pseudo-random value in the interval $[0, 1]$ through the quantized cumulative distribution of H: since the bins can be ordered as a one-dimensional list, a single random number is required. Among all the elements in that class, one is selected randomly.

In limit cases where all elements belong to the same attribute class, or attributes are uniformly distributed, or any other situation where H_1 would be identical to H_2, the method reverts to uniform random sampling over the elements in R_1 and R_2, as in [18].

4.3. Attribute compatibility $\mathcal{C}$

The Boolean compatibility function $\mathcal{C}(\mathbf{r}(\mathbf{u}_i), \mathbf{r}(\mathbf{u}_j))$ determines, on the basis of the attributes $\mathbf{a}(\mathbf{u}_i)$ and $\mathbf{a}(\mathbf{u}_j)$, whether the two rigels $\mathbf{r}(\mathbf{u}_i)$ and $\mathbf{r}(\mathbf{u}_j)$ can be paired. The form of the test is of course a function of the nature of the attributes. If they belong to a finite set of labels, then a minimal test requires the attributes to be identical. For a continuous function, simple thresholding on the difference can be used. However, if an error model of the attributes is available, then the decision can be based on the probability that $\mathbf{a}(\mathbf{u}_i)$ and $\mathbf{a}(\mathbf{u}_j)$ belong to the same distribution.

In any case, the behavior of the algorithm encourages that, in doubt, the compatibility be overestimated. Indeed, in the case of a false positive, the iterative matching method will likely adjust the selection to a geometrically closer compatible point as it progresses. In the limit case, which would be to consider all rigels as mutually compatible, the method would revert to the random sampled ICP of [18].

4.4. Closest compatible point $\mathcal{F}$

The closest point determination operation $\mathcal{F}(\mathbf{r}_a(\mathbf{u}_i), R_b)$ identifies the element $\mathbf{r}_b(\mathbf{u}_{ji}) \in R_b$ that is the closest to $\mathbf{r}_a(\mathbf{u}_i)$ among those that satisfy $\mathcal{C}(\mathbf{r}_a(\mathbf{u}_i), \mathbf{r}_b(\mathbf{u}_j))$. The search for nearest neighbor can gain in efficiency if a proper data structure, which indexes points as a function of attribute, is used to prune the portion of the set that cannot satisfy the compatibility test. In fact, this is a key performance advantage of attribute-based registration.

An important aspect of the proposed algorithm is that the registration distance metric is based on the distance between pairs of individual points of the two images. In most registration methods, a surface is interpolated over the range image data points, and a point is paired with the closest one belonging to the surface, instead of to the nearest neighbor in the original image. This interpolation is required by the viewpoint-dependent nature of the sampling on a surface: in general, the true corresponding point of a given sample lies between the samples in the other image.

Three reasons justify the choice of searching for the nearest neighbor only among the points of the other image: (i) it is a more efficient operation than performing the search over the interpolated surface; (ii) the symmetric (or commutative) design of the algorithm attenuates the impact of the viewpoint-dependent differences in sampling rates [10]; (iii) the goal of the algorithm is to bring the images within a distance in the order of the average inter-point distance of the images, since the result can ultimately be refined using a registration method that interpolates the surface (e.g. [9]). However, attribute interpolation on the surface is possible and efficient search algorithms are currently being investigated.

5. Experiments

As an illustration of the capabilities of the method, an object with symmetry of rotation is chosen for experiments: a painted wooden toy top (Fig. 1). Images are acquired with NRCC's polychromatic range sensor [20]. Here the attributes are the diffuse reflectance coefficients in three channels ($k = 3$), estimated from the range and color image with the method described in [1]. The diffuse reflectance component is computed as part of an integrated geometric and color model building process, of which registration is an element. In this context, these attributes are obtained at no additional computational cost, as opposed to curvature-based attributes.

Figure 1 shows the two original images, with the three computed reflectance coefficients in (a) and (b), and as a shaded surface in (c) and (d). The object was manually rotated by about 45 degrees. With this object, rotation around the symmetry axis is constrained only by the color patterns, thus demonstrating an essential property of the method. Figure 2 illustrates the distribution of attributes in each of the three channels. It must be remembered however that the attributes are used as a single three-dimensional distribution, and not as three one-dimensional distributions as represented here.

One notices from Fig. 2 that the peaks corresponding to each surface tint are wide. This can be explained by the non-uniformity of the surface finish, the measurement noise in the color channels, as well as estimation errors in

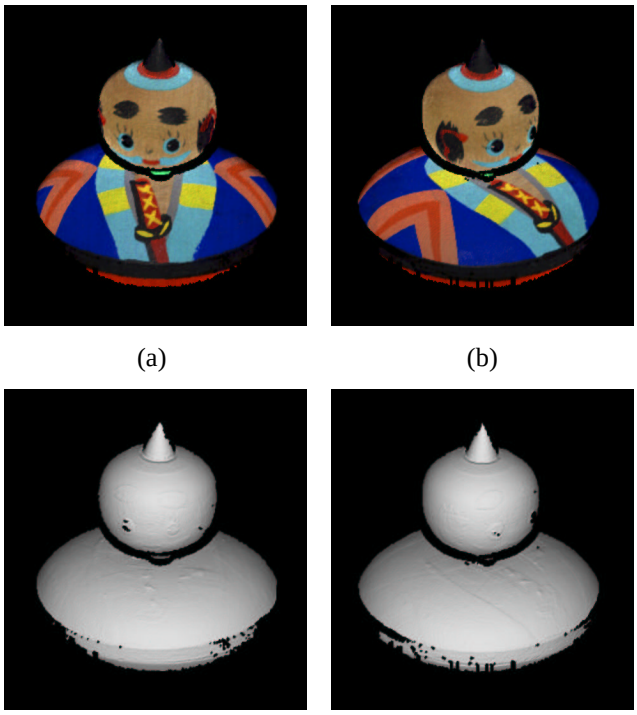

(a) (b) (c) (d)

Figure 1. Test object: (a) image `toy1` (b) image `toy2` (c)(d) shaded views of `toy1` and `toy2`

the reflectance modelling due in part to the non-Lambertian behavior of the surface. The width of the peaks provides a guide for choosing a compatibility metric. As discussed above, it is preferable to overestimate compatibility than to underestimate it: during convergence, improved correspondences might be established as iterations progress. However this situation applies to cases where the object's geometry itself is sufficient to constrain the registration. This condition is not met with this object. Here, the compatibility function was defined to be positive when the distance between attributes is $\leq d_c$ in each of the three channels. Various values of d_c ranging from 8 to 32 were tried, with limited influence over the results. A value of $d_c = 12$ was used in the experiments. The attributes belong to a continuous (albeit quantized to 3×8 bits) function. The sampling distribution H is quantized into $16 \times 16 \times 16$ bins over the range $(0, 0, 0)$ to $(255, 255, 255)$ for the purpose of random sample selection.

The RSICCP algorithm was run on 50 subsets of 100 rigels in each image, using only the identity matrix as an initial estimate, that is, using the actual relative positions of the object displayed in Fig. 1 as a starting point. The best LMS estimation found by RSICCP is shown in Fig. 3(a). The images are superimposed. The geometric registration

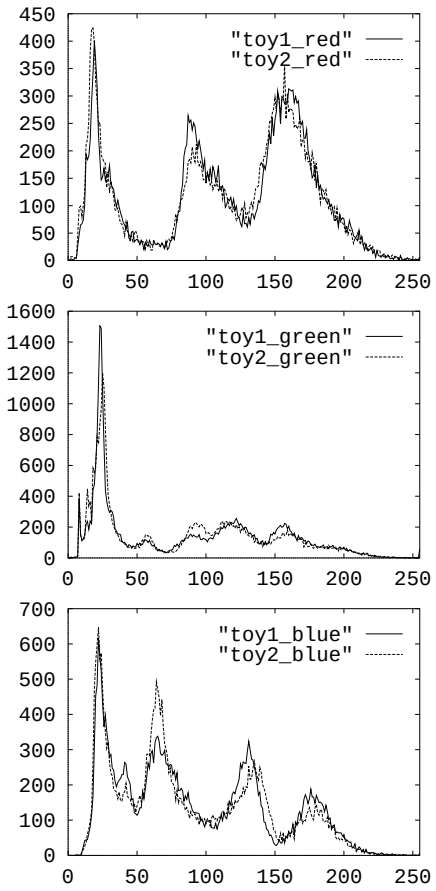

Figure 2. Histograms

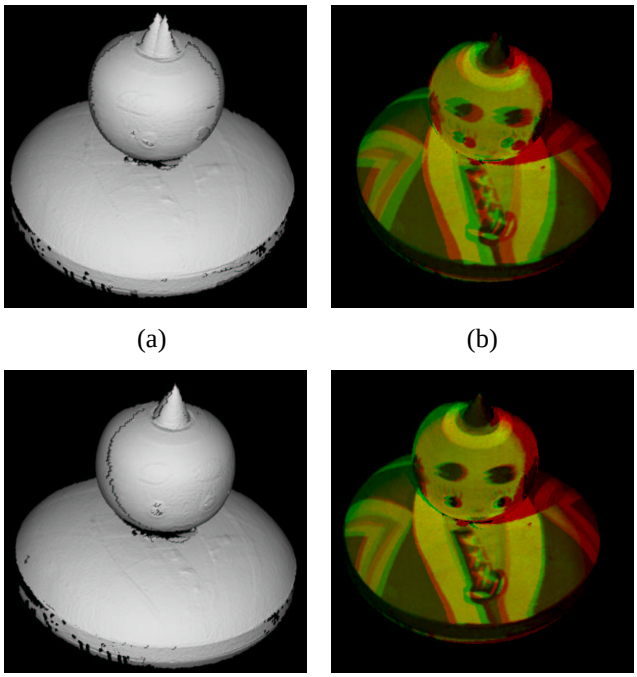

(a) (b) (c) (d)

Figure 3. Results: (a)(b) RSICCP estimation (c)(d) ICCP refinement. In (b) and (d), the original color images are converted in grey levels, and superimposed in two different color channels (red for `toy1`, green for `toy2`).

is off, as can be seen from the conic hat; Fig. 3(b) shows that the colors are also out of alignment, as can be expected from a registration performed only on a small subset of the data.

The ICCP refinement stage significantly improves the geometric registration (Fig. 3(c)). The colors (Fig. 3(d)) are better aligned than at the output of the first stage of the method, but there is a residual error in rotation of about 1 degree, even after 60 iterations of the ICCP. This result was consistent over a number of runs of the algorithm and with variations on sample size as well as d_c. It also seems that the cost function in the ICCP exhibits several local minima.

6. Discussion

The method described here is a general framework that is applicable for the registration of images where useful attributes are computable: colored objects scanned with color-and-range sensor, objects with affixed intensity targets that are easily detected, machined objects with segmentable curvature classes, etc. When attributes are independent of the geometry, such as color, they may allow registration even under residual geometric degrees of freedom, as illustrated in the example of Section 5. Obviously, the benefits of attribute-driven random sampling vary with the attributes nature as well as their distribution. In the best case, it allows the early identification of common regions in both images, thus transforming the problem into a subset-to-model registration problem well suited for the ICP. In the worst case, with uniform attributes or periodic patterns, the method should behave similarly to the simple random-sampled ICP [18].

Registration methods based on the ICP exhibit slow convergence rate if implemented in a straightforward manner. However, because of its structure similar to that of the ICP, the inner loop of the RSICCP is amenable to the acceleration techniques proposed in [4]. The full registration problem must be solved for a set of range images: the method is presented here only for a pair of images, but is easily extended to the case of n images with a framework similar to the one described in [9].

When possible, the particular form of the compatibility function $\mathcal{C}$ should include models of the attributes uncertainty; the decision can then be based on a proper statistical test. However the additional cost imposed by such a tech-

nique may not justify its use in the random sampling stage of the method, but could prove beneficial in the evaluation of the quality of the registration and in its refinement. The biased selection function $\mathcal{H}$ could incorporate preferences that are guided by a priori knowledge of the constraining capability of particular attribute values, or of their distribution on the surface, including a measure of saliency.

Alternative refinement techniques that integrate attribute information are currently being investigated. However, in many circumstances, refinement using the attributes may not be required and one could skip directly to a geometry-only minimization if the object's geometry provides sufficient constraints.

7. Conclusions

This paper described a method for the registration of pairs of range images which uses the information provided by attributes to constrain the pairing of points and select random subsets in a LMS algorithm. It showed an ability to register a rotationally symmetric object based only on the distribution of color patterns. Research is currently under way to further assess the behavior of the algorithm, to improve its performance especially at the refinement level, and to develop efficient data structures to accelerate the closest compatible point determination for more complex forms of compatibility functions.

References

[1] R. Baribeau, M. Rioux, G. Godin, "Color reflectance modeling using a polychromatic laser range sensor", IEEE Trans. on Pattern Analysis and Machine Intelligence, vol. 14, no. 2, Feb. 1992. pp. 263-269.

[2] R. Bergevin, D. Laurendeau, D. Poussart, "Registering range views of multipart objects", Computer Vision and Image Understanding, vol. 61, no. 1, Jan. 1995, pp. 1-16.

[3] P.J. Besl, R.C. Jain, "Invariant surface characteristics for 3D object recognition in range images", Computer Vision, Graphics, and Image Processing, vol. 33, 1986. pp. 33-80.

[4] P. J. Besl, N. D. McKay, "A method for the registration of 3-D shapes", IEEE Trans. on Pattern Analysis and Machine Intelligence, vol. 14, no. 2, Feb. 1992. pp. 239-256.

[5] G. Blais, M.D. Levine, "Registering multiview range data to create 3D computer objects", IEEE Trans. Pattern Analysis Machine Intelligence, vol. 16, no. 10, 1995. pp. 820-824.

[6] P. Boulanger, P. Cohen, "Viewpoint invariant computation of surface curvatures in range images", Proc. Vision Interface 94, Banff, Canada. May 16-20, 1994. pp. 145-154.

[7] J. Feldmar, N. Ayache, "Rigid, affine and locally affine registration of free-form surfaces", Int. J. Computer Vision, vol. 18, no. 2, 1996. pp.99-119.

[8] F.P. Ferrie, M.D. Levine, "Integrating information from multiple views", Proc. IEEE Workshop on Computer Vision, Miami Beach FL, 1987. pp. 117-122.

[9] H. Gagnon, M. Soucy, R. Bergevin, D. Laurendeau, "Registration of multiple range views for automatic 3-D model building", Proc. IEEE Conf. on Computer Vision and Pattern Recognition, Seattle WA, 1994. pp. 581-586.

[10] G. Godin, M. Rioux, R. Baribeau, "Three-dimensional registration using range and intensity information", Proc. SPIE Videometrics III, vol. 2350, Boston, 2-4 Nov. 1994. pp. 279-290.

[11] G. Godin, P. Boulanger, "Range image registration through invariant computation of curvature", Proc. ISPRS Workshop *From Pixels to Sequences*, Zurich, Switzerland, 1995. pp. 170-175.

[12] B.K.P. Horn, "Closed-form solution of absolute orientation using unit quaternions , Journal of the Optical Society of America A, vol. 4 no. 4, April 1987. pp. 629-642.

[13] K. Ikeuchi, K. Sato, "Determining reflectance properties of an object using range and brightness images", IEEE Trans. Pattern Analysis Machine Intelligence, vol. 13, no. 11, Nov. 1991. pp. 1139-1153.

[14] A.E. Johnson, S.B. Kang, "Registration and integration of textured 3-D data", Proc. Int. Conf. on Recent Advances in 3-D Digital Imaging and Modeling, Ottawa, Canada, May 12-15, 1997. pp. 234-241.

[15] O. Jokinen, "Area-based matching for simultaneous registration of multiple 3-D profile maps", Computer Vision and Image Understanding, vol. 71, no. 3, Sept. 1998. pp 431-447.

[16] G. Kay, T. Caelli, "Inverting an illumination model for range and intensity maps", CVGIP: Image Understanding, vol. 59, no. 2, March 1994. pp. 183-201.

[17] N. Ketharnavaz, S. Mohan, "A framework for estimation of motion parameters from range images", Computer Vision, Graphics and Image Processing, vol. 45, 1989. pp. 88-105.

[18] T. Masuda, N. Yokoya, "A robust method for registration and segmentation of multiple range images", CVGIP: Image Understanding, vol. 61, No. 3, May 1995. pp. 295-307.

[19] K. Pulli, "Surface reconstruction and display from range and color data", Ph.D. Thesis, Dept. of Computer Science, University of Washington, 1997.

[20] M. Rioux, "Digital 3-D imaging, theory and applications", Proc. Videometrics III, SPIE vol. 2350, 1994. pp. 2-15.

[21] G. Roth, "Registering two overlapping range images", Proc. Second Int. Conf. on 3-D Digital Imaging and Modeling, Ottawa, Canada, Oct. 4-8, 1999. pp. 191-200.

[22] C. Schütz, T Jost, H. Hügli, "Multi-featured matching algorithm for free-form 3D surface registration", Proc. Int. Conf. Pattern Recognition, Brisbane, Australia, 1998. pp. 982-984.

[23] G. Soucy, F. P. Ferrie, "Motion and surface recovery using curvature and motion consistency", 2nd European Conf. on Computer Vision 1992, Santa Margherita Ligure, May 19-22, 1994. pp. 222-226.

[24] S. Weik, "Registration of 3-D partial surface models using luminance and depth information", Proc. Int. Conf. Recent Advances in 3-D Digital Imaging and Modeling, Ottawa, Canada, May 12-15, 1997. pp. 93-100.

[25] M. Yamamoto, P. Boulanger, J.-A. Beraldin, M. Rioux, "Direct estimation of range flow on deformable shape from a video rate range camera", IEEE Trans. on Pattern Analysis and Machine Intelligence, vol. 15, no. 1, 1993. pp. 82-89.

[26] Z. Zhang, "Iterative point matching for registration of free-form curves and surfaces", Int. Journal of Computer Vision, vol. 13, no. 2, 1994. pp. 119-152.